Timo Dederichs

Time-resolved X-ray Spectroscopy of C-H Bond Activating Transition Metal Complexes

This Page will be Replaced before Printing

Title page logo

Abstract Dummy Page.

To Mama and Papa

List of papers

This thesis is based on the following papers, which are referred to in the text by their Roman numerals.

I Time-resolved Resonsant Inelastic X-ray Scattering reveals how Molecular Orbital Symmetry Alignment enables C-H Activation with Cp*Rh(CO)$_2$ and CpRh(CO)$_2$

II X-ray absorption spectroscopy of a coordinatively unsaturated 3d transition metal complex

Reprints were made with permission from the publishers.

Contents

1. Introduction

Carbon-Hydrogen (C-H) bonds are one of the most stable bonds in nature, making them generally unreactive. On the one hand this is great, as all organic molecules, are based on a backbone of carbon atoms, each typically bonded to hydrogen atoms. That means that hydrocarbons and biomolecules stay intact under normal conditions, so that our body, fuels and plastics do not spontaneously fall apart. On the other side this stability can be a challenge for synthetic chemistry if these bonds need be modified. This is where the field of C-H activation is working on.

But why is this relevant?

C-H activation has the potential to revolutionize the chemical industry. Alkanes, or saturated hydrocarbons, are major constituents of natural gas [1], which is a large and low-cost feedstock which remains unused for chemical synthesis [2] due to their chemical inertness. Until know, there are very few practical processes for converting them directly to more valuable products. Alkanes react at high temperatures, as in a combustion engine, however these reactions only yield the unattractive products carbon dioxide and water. Selective C-H activation and transformation of such unsaturated hydrocarbons offers a power strategy to place chemical groups directly at a desired part in a molecule. Traditional synthetic approaches, like cross-couplings reactions (recognized with the 2010 Noble price in Chemistry) [3, 4, 5], require multiple steps and pre-functionalization to achieve comparable results. By bypassing pre-functionalization, selective C-H activation not only streamlines synthesis, but also reduces the generation of hazardous waste [6, 7], aligning with the principles of green chemistry [8].

So how can C-H bonds be activated?

One approach to activating C-H bonds is using transition metal complexes. Typically these reactions are conducted at high temperatures or in a special solvent, as they require the dissociation of one ligand to form a highly reactive 16 valence electron species. A more energy sustainable approach would be to form the reactive species photo chemically [9, 10], which can be achieved at room temperature. The open coordination site of the low valent metal complex enables the binding of an alkane [11, 12, 13, 14] and subsequently, the activation of one it's C-H bonds [15, 16, 17, 18]. The key intermediate in these

photochemical C-H activation reactions are so-called σ-alkane complexes, in which a C-H bond loosely binds to the metal (see schematic in Figure 1.1).
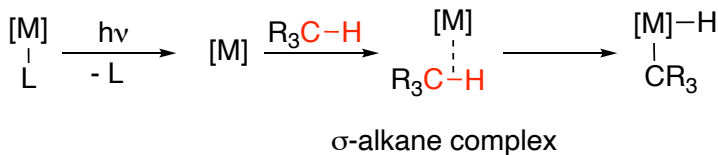
$$\underset{\text{L}}{\overset{\text{[M]}}{|}} \xrightarrow[\text{- L}]{h\nu} \text{[M]} \xrightarrow{R_3C-H} \underset{R_3C\overset{|}{-}H}{\overset{\text{[M]}}{:}} \longrightarrow \underset{\text{CR}_3}{\overset{\text{[M]}-\text{H}}{|}}$$

σ-alkane complex

Figure 1.1. Schematic for photochemical C-H activation. [M] is an example metal complex where a ligand L can be photochemically cleaved.

σ-alkane complexes are short-lived, typically exhibiting lifetimes on the picosecond (ps) timescale. Their electronic properties play a key role in determining whether a metal complex is suitable for C-H activation: The reaction may proceed via oxidative addition, in which the metal is inserted into the C-H bond, or it may terminate at the formation of the σ-alkane complex. Consequently, probing these short-lived intermediates is essential for understanding what determines reactivity of a given transition metal complex.

How can σ-alkane complexes be probed?

Conventional approaches methods like isotope labeling [12] and nuclear magnetic resonance (NMR) spectroscopy [19, 20, 21] have been instrumental in revealing the overall mechanisms in C-H activation. Neutron and X-ray diffraction [22, 23, 24, 25] are decisive for determining the structures of frozen or crystallized σ-alkane complexes. Time-resolved infrared (IR) spectroscopy has proven essential for detecting and structurally characterizing short-lived intermediates during the reaction pathway [18, 16, 26, 27, 28]. However, all these techniques lack the sensitivity to directly probe electronic structure which limits their ability to correlate the underlying electronic interactions with C-H bond reactivity. This were time-resolved X-ray absorption spectroscopy (XAS) and resonant inelastic X-ray scattering (RIXS), which are the main two techniques of this thesis, can be utilized to fill this information gap.

In the following chapters will go into more detail about the background of the electronic structure of transition metal complexes during photochemical C-H activation (Chapter 2) and will have a more detailed look at the methods used in this thesis (Chapter 4). ADD PART about the Papers

2. Theoretical Background

2.1 Molecular Orbital Theory

In order to understand the bonding in organometallic systems, we first have to understand the theoretical background of electron structure in molecules. This strucutre of this section is based on these books [29, 30]. We start of with the time-independent Schrödinger equation, which describes the energy of a system as:

$$\hat{H}\Psi(r) = E\Psi(r), \tag{2.1}$$

where $\hat{H}$ is the Hamilton operator, Ψ is the wavefunction of the system at the position r in space, and E is the total energy of the system. The Hamiltonian is given as the sum of the operator for kinetic energy $\hat{T}_{kin}$ and potential energy $\hat{V}$, which can be rewritten as:

$$\hat{H} = \hat{T}_{kin} + \hat{V}. \tag{2.2}$$

Solving the Schrödering equation in spherical coordinates yields the following wavefunction:

$$\Psi_{n,l,m}(r,\theta,\phi) = R_{n,l}(r)Y_l^m(\theta,\phi), \tag{2.3}$$

which is product of $R_{n,l}(r)$, related to the Laguerre functions, depending only on the distance r, and $Y_l^m(\theta,\phi)$, which is a spherical harmonic, containing all angular information [29]. Here, n is the principle quantum number, l is the angular momentum quantum number, and m is the magnetic quantum number. The Schrödering equation can only be exactly solved for one-electron systems (e.g., H, Li^{2+}). In the specific case of one-electron wavefunctions they are called atomic orbitals (AO). For historical reasons, orbitals with $l = 0$, 1, 2, and 3 are termed s-, p-, d- and f-orbitals, respectively. An electron by a given one-electron wavefunction $\Psi_{n,l,m}$ can be understood as occupying that orbital and referred to as and s-, p-, d- and f-electron.

As for systems with more than one electron the Schrödinger equation cannot be solved, an approximation has to be introduced to the describe the electronic structure for many-electron systems, especially molecules. Molecular orbitals (MOs) can be approximated as a linear combination of atomic orbitals (LCAO ansatz):

$$\psi_i = c_{1i}\phi_1 + c_{2i}\phi_2 + \cdots + c_{mi}\phi_m = \sum_a c_{ai}\phi_a, \tag{2.4}$$

where the index i ranges from 1 to m which is the total number of basis functions. ϕ are the atomic basis functions and c_{ai} are the molecular orbital coefficients. These MOs are one-electron wavefunctions and are orthonormal (i.e. normalized and orthogonal)

$$\langle \psi_i | \psi_j \rangle = \delta_{ij}, \tag{2.5}$$

where $\delta_{ij} = 1$ for $i = j$ and $\delta_{ij} = 0$ for $i \neq j$. The molecular orbital coefficients c_{ai} act as scaling factor of the ath atomic orbital and specify the nature and energy of the orbital ψ_i. They are determined by solving the eigenvalue equation of the effective one-electron Hamiltonian $\hat{H}^{\text{eff}}$ associated to the molecule:

$$\hat{H}^{\text{eff}} \psi_i = \varepsilon_i \psi_i. \tag{2.6}$$

Here, ε_i is the molecular orbital energy of the an electron located in ψ_i, which can be calculated as the expectation value of $\hat{H}^{\text{eff}}$.

$$\varepsilon_i = \langle \psi_i | \hat{H}^{\text{eff}} | \psi_i \rangle \tag{2.7}$$

Before we continue with this formalism, we introduce the overlap integral $S_{\mu\nu}$ between two atomic orbitals ϕ_μ and ϕ_ν:

$$S_{\mu\nu} = \langle \phi_\mu | \phi_\nu \rangle, \tag{2.8}$$

which describes the spatial overlap of two wavefunctions (here in Figure 2.1 the overlap of two 1s orbitals).
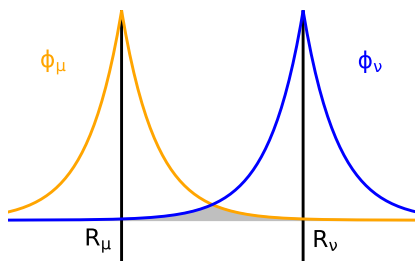
Figure 2.1. Spatial overlap of wavefunctions of two 1s orbitals having the same phase. The atomic orbitals have their origin at R_μ and R_ν. The gray shaded area indicates the overlapping area between the two wavefunctions.

The interaction between two orbitals with each other is quantified in the magnitude of the overlap integral, serving as a powerful tool in the detailed analysis of molecular orbitals. Especially the symmetry of the atomic orbitals is of great importance in dictating whether the overlap integral is zero or not. Figure 2.2 shows an overview of various types of overlap integrals. σ-symmetric orbital overlap is characterized by the absence of nodes along the internuclear axis, whereas π-symmetric overlap contains a single node, and δ-symmetric

contains two nodes along the axis. Nodes along the internuclear axis decrease the overlap between orbitals, which results in a decrease of the overlap integral according to $\sigma > \pi > \delta$. This general rule of thumb is only valid for valence orbitals of atoms from the same row of the periodic table [30] and depends strongly on the spatial extend of the respective atomic orbitals.
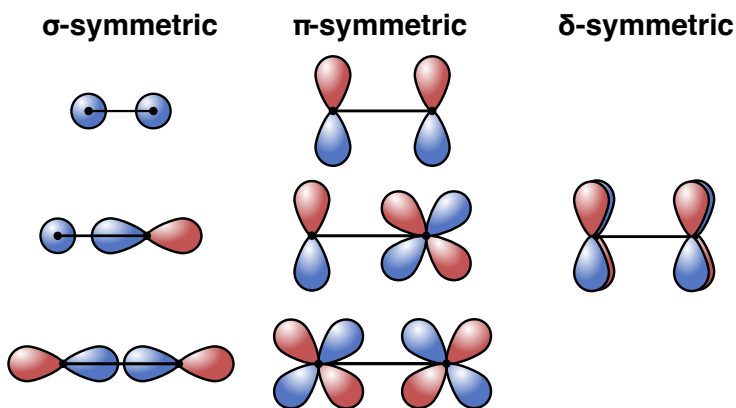
σ-symmetric **π-symmetric** **δ-symmetric**

Figure 2.2. Examples of different types of overlap between atomic orbitals.

Another aspect influencing the overlap, is the principle quantum number n of the atomic orbitals. As n increases, the atomic orbitals become more diffuse which normally decreases the overlap. Moreover, the orbital overlap is highly sensitive to the internuclear distance between atoms as well as to the electronegativity, where less electronegative atoms exhibit more diffuse orbitals. An important exception to the generalization discussed above occurs in transition metal complexes. The 3d orbitals are relatively contracted due to their poor radial extension and ineffective shielding by inner electrons. At typical metal-ligand distances, this contraction reduces their spatial overlap with ligand orbitals. In contrast, 4d and 5d valence orbitals are radially more extend as a result of stronger shielding of the positive charge of their nucleus, and therefore exhibit greater overlap with ligand orbitals. Last, the overlap is very sensitive to the geometry of the molecule.

Coming back to equation 2.4, in order to get the optimum value for the orbital coefficients c the variation principle is applied, which leads to the problem of solving the secular equations (an exact derivation can be found here [30]):

$$\sum_a c_{ai} \left(\hat{H}_{\mu\nu} - \varepsilon_i S_{\mu\nu} \right), \tag{2.9}$$

where $\hat{H}_{\mu\nu}$ is a matrix element of the Hamiltonian and the index i indicates the molecular orbital level. The Hamiltonian is given as:

$$\hat{H}_{\mu\nu} = \langle \phi_\mu | \hat{H}^{\text{eff}} | \phi_\nu \rangle. \tag{2.10}$$

13

The secular equations 2.9 can be express in matrix form as the following:

$$\mathbf{H}\vec{c} = \varepsilon \mathbf{S}\vec{c}. \tag{2.11}$$

This is a matrix eigenvalue problem, which represents the formulation of quantum mechanics by Heisenberg. The advantage of this approach is the transformation of differential equations into an algebraic eigenvalue problem, which can be solved efficiently by computer algorithms. Here, $\mathbf{H}$ is the Hamiltonian matrix of elements $\hat{H}_{\mu\nu}$, $\vec{c}$ is the coefficient vector containing all unknown orbital coefficients c_i, ε is the diagonal matrix of energies ε_i, $\mathbf{S}$ is the overlap matrix containing $S_{\mu\nu}$.

Solving the eigenvalue equation gives the orbital coefficients and makes the construction of MOs according to LCAO ansatz (see equation 2.4). For the example of a degenerate interaction, so two atomic orbitals with the same energy, we get the two following MOs:

$$\psi_1 = \frac{1}{\sqrt{2+2S_{12}}}(\phi_1 + \phi_2) \tag{2.12}$$

$$\psi_2 = \frac{1}{\sqrt{2-2S_{12}}}(\phi_1 - \phi_2) \tag{2.13}$$

Here, ψ_1 is the bonding MO, formed by the in-phase combination of the atomic orbitals ϕ_1 and ϕ_2, whereas ψ_2 is the anti-bonding MO, formed by the out-of-phase combination. They are depicted in a molecular orbital diagram in Figure 2.3a together with the case of nondegenerate interaction (Figure 2.3b). The derivation of the analytic expression of those MOs will not be covered here, but can be found in the literature [30].

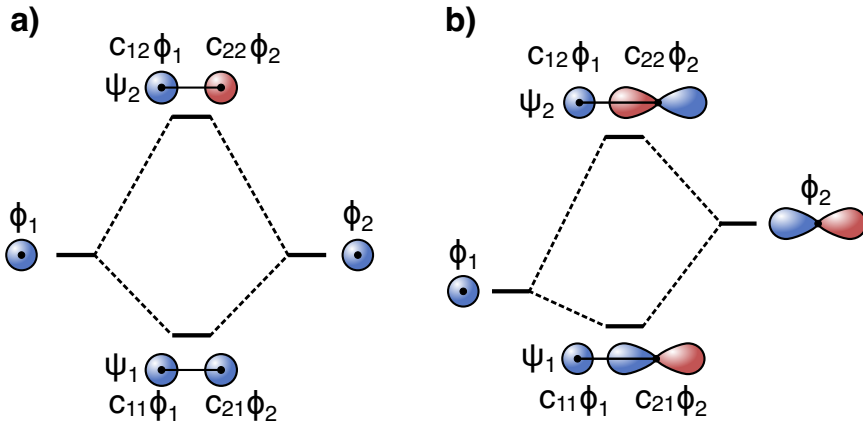*Figure 2.3.* Molecular orbital diagram of a) the degenerate interaction between two atomic s orbitals and b) the non-degenerate interaction between a atomic s and p orbital. The atomic orbitals are denoted as ϕ_1 and ϕ_2 and their in-phase and out-of-phase combination as ψ_1 and ψ_2, respectively. The first index of the orbital coefficients indicates the atom and the second the corresponding MO.

Until here, we have only considered the two-orbital problem, which is extremely powerful as many bonding situations in chemistry can be reduced into this from. General trends of orbital interactions in this picture can be summarized as the following:

1. The upper MO (out-of-phase combination, antibonding) is destabilized more than the lower MO (in-phase combination, bonding).
2. The magnitude of the interaction energy (MO splitting) increases with increasing overlap of the atomic orbitals.
3. In nondegenerate orbital interaction, the magnitude of the interaction energy is inversely proportional to the energy difference of the interacting orbitals. The character of a molecular orbital most closely reflects that of the atomic orbital nearest to it in energy.

To get molecular orbitals of polyatomic species, the same LCAO ansatz (see eqaup 2.4 can be utilized with the sum ranging over all atomic molecules of the atoms in the molecule. Similar to the two-orbital example, only atomic molecules with appropriate symmetry can contribute due to their net overlap. With this key concept introduced, we are now able to utilize molecular orbitals to explain the bonding in metal organic complexes, which will be the topic of the next section.

2.2 Organometallic Bonding

Organometallic complexes comprise a vast array of metals, oxidation states, and ligands and thus enable a wide variety of structures and unique bonding motives, which provide the foundation for the reactivity and stability. Thus, it is important to introduce the fundamental principles to understand their unique behavior. We will focus here in particular on organometallic complexes using transition metals. A complete and detailed description of the underlying interactions can be found in the literature [10, 30].

2.2.1 Types of Organometallic Bonding

In general, a transition metal complex consists of a central transition metal atom which is surrounded by molecules or atoms which are called ligands. An important formalism in organometallic bonding is the determination of the number of electrons of the ligand involved in the bonding to the metal. This interaction are to large extend Lewis acid-base (electron acceptor and donor) interactions, in which the metal often acts as a Lewis acid and the ligand as a Lewis base. This interaction can occur through different modes of orbital overlap between the ligand and metal, with the two most fundamental being σ-bonding and π-bonding, which have there name due to the symmetry requirements of the orbitals involved in these interactions (see Figure 2.2). These different bonding motives are schematically shown in Figure 2.4.
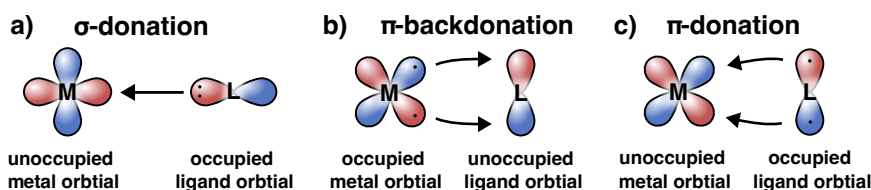
a) σ-donation   **b) π-backdonation**   **c) π-donation**

| unoccupied
metal orbtial | occupied
ligand orbtial | occupied
metal orbtial | unoccupied
ligand orbtial | unoccupied
metal orbtial | occupied
ligand orbtial |

Figure 2.4. Schematic and generalized orbital interactions for a) σ-donation, b) π-donation, and c) π-backdonation in organometallic complexes.

In σ-bonding, the interaction between the ligand and metal arises from the overlap of a filled ligand orbital with metal orbital along the internuclear axis. In most case electron density from a ligand lone pair (e.g. in phosphines or amines) is donates into an empty metal orbital, increasing thereby the electron density at the metal center. Ligands exhibiting such bonding are called σ-donors. A more special case of σ-bonding will be discussed in greater detail in section 2.2.2.

In π-bonded ligands, the involved orbitals of the ligand and metal are oriented perpendicular to the internuclear axis. The interaction between can be divided into π-donation and π-back-donation. We focus first on π-backdonation, in which electron density is transferred from an occupied metal d-orbital into an unoccupied ligand orbital. This interaction is extremely important for the stabilization of complexes with metals in a low formal oxidation states. Most prominent examples for this interaction are carbon monoxide (CO) or nitrosyl cation (NO^+) which act as strong electron acceptors using their unoccupied π^*-orbitals. This donation of electron density from the metal to the π^*-orbital is know as "backbonding". This destabilizing interaction is more than compensated by the reduced electron density at the metal. In π-donation, electron density is transferred from an occupied ligand orbital into an empty metal d-orbital, analogous to σ-donation but involving orbitals oriented perpendicular to the metal-ligand axis. Typical π-donor ligands are aromatic systems like arenes. In general, these different bonding motives can appear in a single ligand, as long as the symmetry requirements are met for the interactions. However, there relative magnitude is influenced by the electronic structure of the ligand itself.

2.2.2 Sigma-Complexes

A special type of metal-ligand interaction occurs in so-called σ-complexes, in which neutral molecules like dihydrogen, alkanes, silanes and boranes are bound through their H-H, C-H, Si-H or B-H bonds, respectively. Here, we will focus mainly on the case of σ-alkane complexes as they are the key intermediate in activation of C-H bonds via oxidative addition. The C-H bond binds to the transition metal complex in a combination of two charge transfer interactions (see Figure **??** SHOULD I REALLY DO THIS?), which were first

conceptualized on an orbital level by Saillard and Hoffmann [31]. On the one hand, electron density is donated via ligand-to-metal charge transfer (LMCT) from the occupied C-H σ-orbital to unoccupied metal d-orbitals. On the other hand, electron density is donated in parallel from occupied metal d-orbitals to the unoccupied C-H σ^*-orbital (metal-to-ligand charge transfer, MLCT), acting in the opposite direction. These interactions resemble σ-donation and π-backbonding, respectively. The combination of this bidirectional interactions weakens the C-H bond, thereby facilitating C-H activation. Modulation of the metal center's electronic structure plays an important role in enabling the formation of such intermediates and ultimately governs their reactivity in subsequent oxidative addition steps.

2.3 Photochemical C-H Activation using Transition Metal Complexes

- examples of C-H activation, small historical back ground
- other mechanisms besides C-H activation via sigma complex formation and oxidative addition
- reactivity in C-H activation, Hartwig trends, hoffmann sailard explained in detail

STILL WRITE THIS STUFF

3. Electronic Structure Methods

In the previous chapter, the general concept of MO theory was introduced, which allows the understanding of chemical bonding based on its electronic structure. Until here, the exact energy of these orbitals has been only partially covered. In order to change this, theoretical electronic structure methods are introduced to calculate those energies, which enable us to calculate spectra allowing for comparison with experimental observables. The equations are taken from literature textbooks [32, 33], which describe their derivation in greater detail.

3.1 Hartree-Fock Methods

3.1.1 The Electronic Hamiltonian

The basis of calculating the energy of a system is the Schrödinger equation (eq. 2.1 introduced in section 2.1, consisting of the Hamiltonian $\hat{H}$ and the wavefunction Ψ. Until here, only the general form of the Hamiltonian has been introduced in equation 2.2, which can be further dissected into kinetic and potential energies of the nuclei and electrons:

$$\hat{H} = \hat{T}_e + \hat{T}_N + \hat{V}_{ee} + \hat{V}_{eN} + \hat{V}_{NN}, \tag{3.1}$$

where $\hat{T}$ and $\hat{V}$ are the operators for kinetic and potential energy for electrons e and nuclei N. Thus the terms $\hat{V}_{eN}, \hat{V}_{ee}$, and $\hat{V}_{NN}$ describe the electron-nuclei attraction, electron-electron repulsion and nuclei-nuclei repulsion, respectively. This Hamiltonian provides a formally exact description, however solving the corresponding Schrödinger equation is intractable due to the simultaneous treatment of all particles. A key approximation to circumvent this issue is the Born-Oppenheimer approximation [34]. As nuclei are much heavier than electrons, they move more slowly. Thus it can be assumed that electrons move in a field of fixed nuclei. Within this approximation, the kinetic energy operator for nuclei $\hat{T}_N$ can be neglected and the nuclei-nuclei repulsion $\hat{V}_{NN}$ can be considered to be constant. The remaining terms of equation 3.1 are summarized as the electronic Hamiltonian $\hat{H}_{elec}$ and can be written as the following in its operator form:

$$\hat{H}_{elec} = \underbrace{-\sum_{i=1}^{A} \frac{1}{2}\nabla_i^2}_{\hat{T}_e} + \underbrace{\sum_{i=1}^{A}\sum_{j>i}^{A} \frac{1}{r_{ij}}}_{\hat{V}_{ee}} - \underbrace{\sum_{i=1}^{A}\sum_{N=1}^{B} \frac{Z_N}{r_{iN}}}_{\hat{V}_{eN}}. \tag{3.2}$$

Here, ∇^2 is the Laplace operator, r_{ij} is the distance between the electrons i and j, r_{ij} is the distance between electron i and nucleus N with its atomic number Z_N. Solving the Schrödinger equation for the electronic Hamiltonian, yields the electronic energy as a function of the position of the nuclei $E_{elec}(R)$ (potential energy surface), on which the nuclei move. The total energy E_{tot} can then be calculated by adding the V_{NN} term afterwards, as it has not direct influence on the wavefunction. This assumption directly introduces the adiabatic approximation, which assumes that the nuclear dynamics remain confined to a single electronic state, neglecting couplings to different states. As a consequence no electronic surface transitions are possible.

3.1.2 The "Correct" Wavefunction

In the previous chapter we have manly focused on the one-electron wavefunctions which give access to molecular orbitals of a system. In this chapter, we will take a step back and reconsider what the correct choice of the wavefunction is to describe systems using the Schrödingner equation. The basis for construction of the many-electron wavefunction is the LCAO ansatz introduced in section 2.1, which allows the construction of molecular orbitals on the basis of atomic basis functions. One approach for these atomic basis functions are so-called Slater functions, which are the solutions of the H atom. They are of the type:

$$\phi = Y_l^m(\theta, \phi) \cdot r^{n-1} \exp\frac{-\zeta \cdot |r|}{n}, \tag{3.3}$$

where $Y_l^m(\theta, \phi)$ are the spherical harmonics, n, l, m are the quantum numbers, and ζ is a constant related to the effective charge of the nucleus. However, their integration is very expensive and numerically problematic. Thus, other easier to integrate functions need to be utilized. For molecules, the solution is to use spherical Gaussian functions of the form:

$$\phi = Y_l^m(\theta, \phi) \exp(-\zeta \cdot r^2). \tag{3.4}$$

In contrast to Slater functions, calculations using Gaussian is computational inexpensive (Gaussian product theorem) and the integrals involving them can be solved analytically. Their main drawback is the wrong description of the short- and long-range behavior (to low intensity close to the nucleus and to low intensity at large distances from the nucleus). The solution to this, are so-called contracted Gaussians type orbitals (CGTOs), which are a linear combination of typical 2 to 10 primitive Gaussians type orbitals (PGTOs):

$$\phi^{\text{CGTO}} = \sum_i^{\approx 2-10} c_i \phi_i^{\text{PGTO}}(\zeta_i) \tag{3.5}$$

Until here, the approaches were only solutions for one-electron wavefunctions. The simplest approximation to approach many-electron systems is the so-called Hartree ansatz, which gives the wavefunction of a many-electron system as a combination of individual one electron functions (also called Hartree product) which is given as:

$$\Psi^{\mathrm{HP}} = \phi_1(1)\phi_2(2)\cdots\phi_N(N), \tag{3.6}$$

for an N-electronic systems with each electron in their individual state. In the Hartree product, the electrons are treated as independent particles that interact only through an average or "mean-field" potential generated by the presence of all other electrons. We will return to this issue later in the chapter. Beyond this mean-field approximation, the Hartree product suffers from two additional shortcomings. First, because the electrons are explicitly assigned to specific orbitals, the wavefunction does not satisfy the required antisymmetry condition for fermions (particles with a spin $= n + \frac{1}{2}$). Second, this formulation incorrectly renders the electrons distinguishable, whereas they are fundamentally indistinguishable particles. The indistinguishability and antisymmetry of electrons is implemented by expression of the wavefunction as a Slater determinant:

$$\Psi^{\mathrm{SD}} = \frac{1}{\sqrt{N!}} \begin{vmatrix} \phi_1(1) & \phi_1(2) & \cdots & \phi_1(N) \\ \phi_2(1) & \phi_2(2) & \cdots & \phi_2(N) \\ \vdots & \vdots & \ddots & \vdots \\ \phi_N(1) & \phi_N(2) & \cdots & \phi_N(N) \end{vmatrix} = |\phi(1)\phi(2)\cdots\phi(N)\rangle \tag{3.7}$$

3.1.3 The Hartree-Fock Procedure

With now a valid wavefunction and Hamiltonian, we can now proceeding to calculate the energy of a system. As discussed previously, an exact solution to the Schrödinger equation can only be obtained for one-electron systems. For many-electron systems, approximate solutions must be employed. One approach is based on the variational principle, which states that every approximate solution of the wavefunction possesses an energy which always exceeds the exact energy E_0. This approximate energy can be optimized by iteratively trying to minimize the energy by optimizing the orbitals (one-electron wavefunctions) which are used to construct the many-electron wavefunction. In order to do so, we need to transform the Schrödinger equation into a matrix eigenvalue problem, which can iteratively be solved in computer algorithms. The first step is the dissection of the electron Hamiltonian (see eq. 3.2) into one-electron $\mathcal{O}_1$ ($\hat{T}_e$ and $\hat{V}_{eN}$) and two-electron $\mathcal{O}_2$ ($\hat{V}_{ee}$) operators. For the one-electron operators, integration is performed only over the orbitals associated with the i-th electron, while contributions from all other orbitals vanish due to their integrals resulting to unity. The two one-electron operators are often combined into a single operator, denoted as h. The two-electron operator

can be further decomposed into the Coulomb integral J_{ij}, which describes the classical Coulomb repulsion between two electrons i and j, and the exchange integral K_{ij}, which has no classical analogue. The exchange integral arises purely from quantum mechanics, as a consequence of the indistinguishability of fermions and the antisymmetry requirement of the wavefunction. This phenomenon can be understood as follows: Each electron creates an exchange hole in its vicinity, a region from which other electrons of the same spin are excluded. This behavior is a manifestation of the Pauli-Principle. A detailed derivation of these terms can be found here [33]. Using these new integrals the energy of a Slater determinant can be written as:

$$E_{elec} = \sum_i^A h_i \sum_{i<j}^{A,A} J_{ij} - K_{ij} \tag{3.8}$$

According to this equation, each electron contributes an attraction to the nuclei and possesses a certain kinetic energy, both described by the one-electron operator h. Furthermore, each unique pair of electrons contributes a Coulomb repulsion term J, which is subsequently corrected by the exchange interaction K for pairs of electrons with the same spin. For the purpose of deriving at an expression to be used in the variational principle, it is convenient to transform the energy expression in 3.8 in terms of its operator form, which is called the Fock operator:

$$f(1) = h(1) + \sum_i^A \mathcal{J}_i(1) - \mathcal{K}_i(1). \tag{3.9}$$

This new one-electron operator obtains a set of A (number of electrons) interdependent eigenvalue problems:

$$\{f(i)\psi_i(i) = \varepsilon_i \cdot \psi_i(i)\}. \tag{3.10}$$

Using the definition of the molecular orbitals via the LCAO ansatz (see equation 2.4) and inserting it into equation 3.10 we yield:

$$f(i) \sum_a^{M_{basis}} c_{ai}\phi_a = \varepsilon_i \sum_a^{M_{basis}} c_{ai}\phi_a, \tag{3.11}$$

where M_{basis} is the amount of atom centered basis functions. Multiplying from the left by a specific basis function and integrating yields the Roothaan-Hall equations [35]. These are the Hartee-Fock equations in the atomic orbital basis. They can be collected for all M_{basis} equations in a matrix notation:

$$\mathbf{FC} = \mathbf{SC}\varepsilon, \tag{3.12}$$

with

$$\mathbf{F}_{\mu\nu} = \langle \phi_\mu | f(1) | \phi_\nu \rangle \quad \text{and} \quad \mathbf{S}_{\mu\nu} = \langle \phi_\mu | \phi_\nu \rangle \tag{3.13}$$

3.1.4 Post Hartree-Fock Methods

3.2 Density Functional Theory

Write some stuff about DFT here, THIS is new

4. X-ray Based Spectroscopy Methods

In this chapter, the theoretical basics behind X-ray absorption spectroscopy (XAS) and resonant inelastic X-ray scattering (RIXS), which are the main experimental techniques used in this thesis, will be investigated. Both techniques can be used to investigate the local, element specific, electronic structure. This is of great advantage in comparison to conventional electronic spectroscopies like UV/Vis where the signals are broad and overlap with solvent bands, making it difficult to attribute them to distinct orbital contributions.

4.1 Quantum Formulation of X-ray Interactions with Matter

X-rays interact with matter in through a variety of processes, each of them having different purposes in research or medical applications. Here, we will focus only on the interaction leading to X-ray absorption as this is the underlying process in the experimental techniques used in this thesis. This process involves an excitation of a core electron through the energy transfer of a photon to a bound electron, which is better known as the photoelectric effect CITATION. To calculate and understand the underlying transitions of this process, the quantum mechanical description of this interaction will be discussed in the following section.

4.1.1 Basic Premise

The quantum mechanical description of the photon-matter interactions has its roots in a paper by Kramers and Heisenberg in 1925 [36], written just prior to the formal establishment of quantum theory. Their central idea was that the interaction between photons and matter can be treated as a weak perturbation of the matter's equilibrium state [37]. As a results, photons act as a probe of the unperturbed ground state of matter. To model this perturbation, a Hamiltonian is required describing the interaction of an electromagnetic field with the electron charge and spin. A derivation of the complete interaction Hamiltonian can be found in the literature [37]. For simplicity, we consider only the most dominant terms which are given as:

$$\hat{H}_{int} = \underbrace{\frac{e^2}{2m_e}\hat{A}^2}_{\substack{\text{Thomson} \\ \text{scattering}}} + \underbrace{\frac{e}{m_e}\hat{p}\cdot\hat{A}}_{\substack{\text{photoelectric} \\ \text{transitions}}} , \tag{4.1}$$

where e is the elementary charge, m_e the electron mass, $\hat{A}$ is the time-dependent vector potential and $\hat{p}$ the momentum, given in operator form. The vector potential $\hat{A}(\mathbf{r},t) = \hat{A}^{ab} + \hat{A}^{em}$ can cause absorption (and thereby photon destruction) or emission (through photon creation) [37]. If the term depends linearly on $\hat{A}$, it describes processes in which a photon is either created or annihilated, but not both simultaneously. In contrast, if the term depends quadratically on $\hat{A}$, it allows for both photon creation and annihilation, corresponding to scattering processes.

The essence of the description of electronic excitations lies in the assumption that the system is mostly time independent and that the time evolution can be approximate by a weak perturbation. This concept is used in time-dependent perturbation theory where the total Hamiltonian can be separated into two parts $\hat{H} = \hat{H}_0 + \hat{H}'$ where the $\hat{H}'$ acts a weak time-dependent perturbation of the stationary $\hat{H}_0$. This is justified here as the interaction process with a single photon is so fast ($<1\,\text{as}$) that it is not affected by other atomic effects witch occur on longer timescales. This relative speed comparison is the same concept as in the Born-Oppenheimer approximation [34]. Using the quantization of the electromagnetic field introduced by Dirac in 1927 [38], this leads to the Kramers-Heisenberg-Dirac perturbation theory.

4.1.2 The Kramers-Heisenberg-Dirac Formula

According to the Kramers-Heisenberg-Dirac (KHD) perturbation theory, the time-dependent electromagnetic field induces a transitions from an initial state $|i\rangle$ to a final state $|f\rangle$. Both states include electronic and photonic components, and the transition can be envisioned as proceeding through a multiple steps. First, the electronic and photon parts of the system are decoupled, so that the electronic ground state evolves according to the time-independent Hamiltonian. Second, the interaction takes place, when the electronic state is perturbed by the interaction Hamiltonian $\hat{H}_{int}$ (see eq. 4.1) generating a new state $|f\rangle$. This transition can be written as $\langle f|\hat{H}_{int}|i\rangle$. Third, the electronic excited state evolves again according to the time-independent Hamiltonian. In second order, the transition is made through an intermediate state m, which gives $\langle f|\hat{H}_{int}|m\rangle \langle m|\hat{H}_{int}|i\rangle$. The analogue formulation can be made for higher order of perturbations, however we stop here after the second order term, which can be then formulated as the Kramers-Heisenberg-Dirac (KHD) formula, which is the starting point of quantitative calculation of electronic X-ray processes under the assumption of the Born-Oppenheimer approximation [37]. The tran-

sition probability $\mathcal{W}_{if}$ from a state i to a state f is given as:

$$\mathcal{W}_{if} = \frac{2\pi}{\hbar} \left| \underbrace{\langle f|\hat{H}_{int}|i\rangle}_{1^{st}} + \underbrace{\sum_m \frac{\langle f|\hat{H}_{int}|m\rangle \langle m|\hat{H}_{int}|i\rangle}{\mathcal{E}_i - \mathcal{E}_m}}_{2^{nd}} \right|^2 \rho\left(\mathcal{E}_f\right) \delta\left(\mathcal{E}_f - \mathcal{E}_i\right), \quad (4.2)$$

where $\hat{H}_{int}$ is the interaction Hamiltonian, $|i\rangle$, $|m\rangle$ and $|f\rangle$ are the wavefunctions of the initial, intermediate and final state with their respective energies $\mathcal{E}_i$, $\mathcal{E}_m$ and $\mathcal{E}_f$, $\rho(\mathcal{E}_f)$ is the density of states of final states, and δ is the Dirac δ-function conserving the energy. The first term of the matrix element is better known as "Fermi's golden rule" [39]. The second term describes transitions from the initial state i to the finale state f over a range of possible intermediate states m. Based on this equation, we will discuss in the following sections the transition rate and cross-sections of the processes in X-ray absorption spectroscopy and Resonant inelastic X-ray scattering.
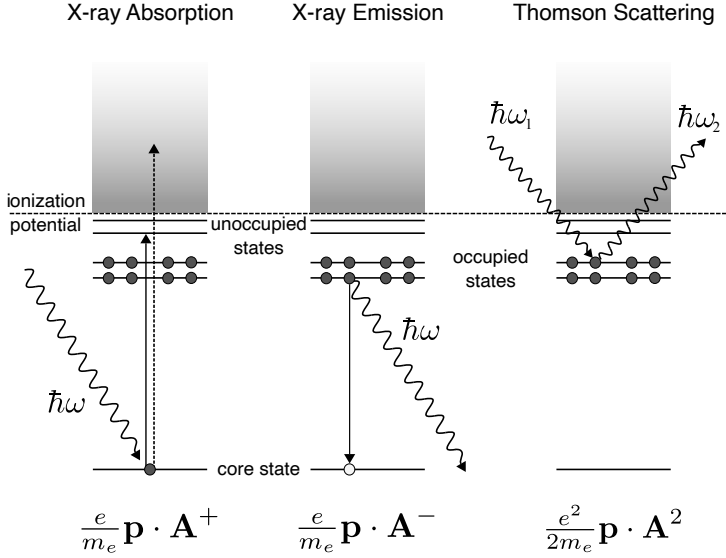

Figure 4.1. Schematic of the first order quantum mechanical process upon interaction of X-rays with matter. Electrons are shown as filled circles, holes as open circles. The operators for the processes are shown below.

Using only the first order term of the KHD equation (eq. 4.2), leads to the quantum mechanical description of X-ray absorption, X-ray emission and X-ray Thomson scattering, illustrated in Figure 4.1, along with their respective interaction Hamiltonian. In X-ray absorption or emission the X-ray photon is absorbed (destroyed) or emitted (created). This is described by the destruction operator $\hat{A}^+$ or the creation operator $\hat{A}^-$, respectively. Thomson scattering

does neither destroys or creates photons and can occur as an elastic or inelastic process. In the following, we will discuss the underlying concepts of X-ray absorption in greater detail.

4.2 X-ray Absorption Spectroscopy

The strongest interaction of X-rays with matter is X-ray absorption. In this process, the incident electric field couples to a core electron, resulting in the absorption of the photon and the transfer of its energy to the electron, which is thereby promoted to an unoccupied level or ejected from the system if the incidence energy is larger than the ionization potential. Both processes are depicted in Figure 4.1 (solid and dashed line). Measuring the photon energy dependent cross section, which is the sum of all photoemission cross sections of orbitals with energy lower than the photon energy, is the main essence of X-ray absorption spectroscopy (XAS). This cross section changes smoothly with photon energy, decreasing with increasing photon energy (shell specific photoemission cross section increases with photon energy), and exhibits sharp so-called absorption edges, where the photon energy matches resonant excitations.
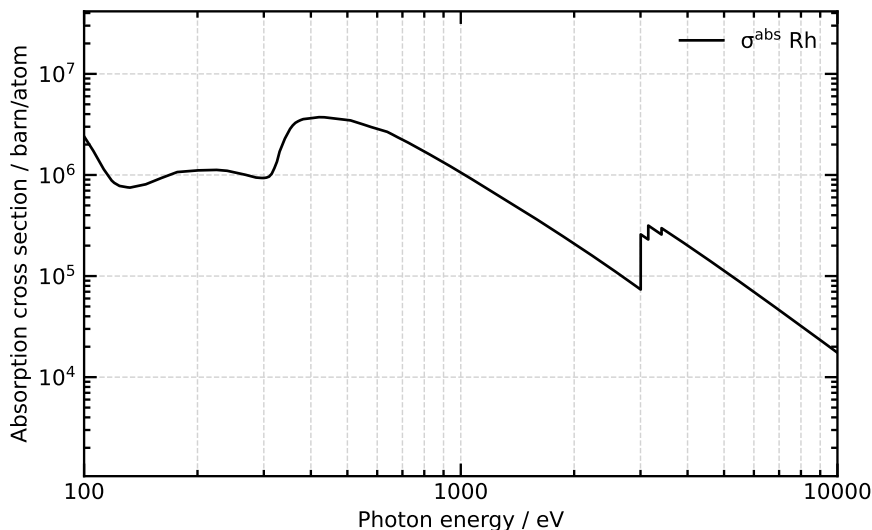
Figure 4.2. Energy dependent X-ray absorption cross section for Rh. The cross sections were calculated from atomic scattering factors from literature [40].

Excitations which exceed resonance excitations in energy can arise from multi-electron excitations, and in the case of molecular or condensed matter due to back scattering of photoelectrons from neighboring atoms. This part of the

spectrum is called extended X-ray absorption fine structure (EXAFS) and will not be discussed here in detail. We will focus here on the resonant near absorption fine structure (NEXAFS) part of XAS, which corresponds to excitations of core electrons to empty valence orbitals, which makes it sensitive to the bonding environment.

To get back to the quantum mechanical description, we utilized the first order term of the KHD equation (4.2 which gives the transition rate for X-ray absorption:

$$\mathcal{W}_{if}^{abs} = \frac{2\pi}{\hbar} \left| \langle f | \hat{H}_{int} | i \rangle \right|^2 \rho\left(\mathcal{E}_f\right) \delta\left(\mathcal{E}_f - \mathcal{E}_i\right). \tag{4.3}$$

with $\hat{H}_{int} = e\mathbf{r} \cdot \hat{E}$, which is a combination of the dipole operator $e\,\mathbf{r}$ and the field operator $\hat{E}$ which can analogously to vector potential $\hat{A}$ can destroy $(\hat{E}^+)$ or create $(\hat{E}^-)$ photons. Until here, the electric field operator $\hat{E}$ depends on the wave vector $\mathbf{k}$, according to

$$E(\mathbf{r},t) = E_0 e^{i(\mathbf{k}\cdot\mathbf{r} - \omega t)}, \tag{4.4}$$

where $\mathbf{r}$ is the position vector, ω is the angular frequency and t is the time. In the dipole approximation, the exponential can be expanded as

$$e^{i\mathbf{k}\cdot\mathbf{r}} = 1 + i\mathbf{k}\cdot\mathbf{r} + \cdots \simeq 1, \tag{4.5}$$

which makes the electric field uniform across the interaction region. As a result, the interaction Hamiltonian $\hat{H}_{int}$ reduces to the dipole operator, and dipole-allowed transitions – subject to the selection rule $\Delta L = \pm 1$ – dominate the transitions. To get the cross section for the X-ray absorption process, the transition rate per unit time $\mathcal{W}_{if}^{abs}$ has to be normalized by the incident photon flux Φ_0

$$\sigma^{abs} = \frac{\mathcal{W}_{if}^{abs}}{\Phi_0} \qquad \text{with} \qquad \Phi_0 = \frac{cn_0}{V} = \frac{2\varepsilon_0 c E_0^2}{\hbar\omega}, \tag{4.6}$$

where ε_0 is the electric field constant, c the speed of light and E_0 the amplitude of the electric field. The photon flux Φ can be imagined as the number of photons n_0 flowing with the speed of light c through a specific volume V.

Following the creation of a core hole through photon absorption, the system stabilizes by spontaneously filling the vacancy. The core hole is filled by an electron form a higher energy level which results in the release of energy. This energy can be either transferred to a valence electron which is ejected from the atom (Auger-Meitner decay) or by the emission of a photon (fluorescence). The ratio of these two decay channels varies with the atomic number Z, with Auger-Meitner decay being favored for lighter elements and fluorescence for heavier elements [41]. The final states reached through these two channels are distinct, meaning that they do not interfere. Consequently, the individual decay rates for X-ray emission Γ^X and for Auger-Meitner decay Γ^{AM} can be summed to give total decay rate Γ:

$$\Gamma = \Gamma^X + \Gamma^{AM} \tag{4.7}$$

The finite lifetime of the electronic excited states results in a natural broadening, also known as lifetime broadening. This is a result of the Heisenberg uncertainty principle [42], which, in its energy-time relation, refers the lifetime to its uncertainty in energy

$$\Delta E \Delta t \geq \frac{\hbar}{2},$$

(4.8)

where ΔE is the uncertainty in energy and Δt is the uncertainty in time. As the decay of electronic excited state occurs exponentially in time, the corresponding lineshape are Lorentzian and Γ represents the Lorentzian FWHM.

4.3 Resonant Inelastic X-ray Scattering

4.4 Time-resolved Spectroscopy

4.5 X-ray Sources

4.5.1 Synchrotron Radiation

4.5.2 Free Electron Lasers

5. Results

5.1 Paper I: Time-resolved Resonsant Inelastic X-ray Scattering reveals how Molecular Orbital Symmetry Alignment enables C-H Activation with Cp*Rh(CO)$_2$ and CpRh(CO)$_2$

6. Discussion and Outlook

References

[1] Jay A Labinger and John E Bercaw. Understanding and exploiting c–h bond activation. *Nature*, 417(6888):507–514, 2002.

[2] Robert G Bergman. C–h activation. *Nature*, 446(7134):391–393, 2007.

[3] NoblePrize.org. The nobel prize in chemistry 2010, 2010.

[4] Akira Suzuki. Cross-coupling reactions of organoboranes: An easy way to construct cï£¿c bonds (nobel lecture). *Angewandte Chemie International Edition*, 50(30):6722–6737, 2011.

[5] Ei-ichi Negishi. Magical power of transition metals: Past, present, and future (nobel lecture). *Angewandte Chemie International Edition*, 50(30):6738–6764, 2011.

[6] Torben Rogge, Nikolaos Kaplaneris, Naoto Chatani, Jinwoo Kim, Sukbok Chang, Benudhar Punji, Laurel L Schafer, Djamaladdin G Musaev, Joanna Wencel-Delord, Charis A Roberts, et al. C–h activation. *Nature Reviews Methods Primers*, 1(1):43, 2021.

[7] Karen I Goldberg and Alan S Goldman. Large-scale selective functionalization of alkanes. *Accounts of chemical research*, 50(3):620–626, 2017.

[8] Toryn Dalton, Teresa Faber, and Frank Glorius. C–h activation: toward sustainability and applications. *ACS Central Science*, 7(2):245–261, 2021.

[9] Bruce A Arndtsen, Robert G Bergman, T Andrew Mobley, and Thomas H Peterson. Selective intermolecular carbon-hydrogen bond activation by synthetic metal complexes in homogeneous solution. *Accounts of chemical research*, 28(3):154–162, 1995.

[10] John F Hartwig. *Organotransition Metal Chemistry: From Bonding To Catalysis*. University Science Books, 2009.

[11] Chris Hall, William D Jones, Roger J Mawby, Robert Osman, Robin N Perutz, and Michael K Whittlesey. Matrix isolation and transient photochemistry of ruthenium complex ru (dmpe) 2h2: characterization and reactivity of ru (dmpe) 2 (dmpe= me2pch2ch2pme2). *Journal of the American Chemical Society*, 114(19):7425–7435, 1992.

[12] William D Jones. Isotope effects in c- h bond activation reactions by transition metals. *Accounts of chemical research*, 36(2):140–146, 2003.

[13] Robert H Crabtree and Douglas G Hamilton. Hh, ch, and related sigma-bonded groups as ligands. In *Advances in organometallic chemistry*, volume 28, pages 299–338. Elsevier, 1988.

[14] Kristof M Altus and Jennifer A Love. The continuum of carbon–hydrogen (c–h) activation mechanisms and terminology. *Communications Chemistry*, 4(1):173, 2021.

[15] L Anders Hammarback, Benjamin J Aucott, Joshua TW Bray, Ian P Clark, Michael Towrie, Alan Robinson, Ian JS Fairlamb, and Jason M Lynam. Direct observation of the microscopic reverse of the ubiquitous concerted metalation

deprotonation step in c–h bond activation catalysis. *Journal of the American Chemical Society*, 143(3):1356–1364, 2021.

[16] Tianquan Lian, Steven E Bromberg, Matthew C Asplund, Haw Yang, and CB Harris. Femtosecond infrared studies of the dissociation and dynamics of transition metal carbonyls in solution. *The Journal of Physical Chemistry*, 100(29):11994–12001, 1996.

[17] Steven E Bromberg, Tianquan Lian, Robert G Bergman, and Charles B Harris. Ultrafast dynamics of cp* m (co) 2 (m= ir, rh) in solution: The origin of the low quantum yields for c- h bond activation. *Journal of the American Chemical Society*, 118(8):2069–2072, 1996.

[18] Steven E Bromberg, Haw Yang, Matthew C Asplund, T Lian, BK McNamara, KT Kotz, JS Yeston, M Wilkens, H Frei, Robert G Bergman, et al. The mechanism of a ch bond activation reaction in room-temperature alkane solution. *Science*, 278(5336):260–263, 1997.

[19] Graham E Ball, Christopher M Brookes, Alexander J Cowan, Tamim A Darwish, Michael W George, Hajime K Kawanami, Peter Portius, and Jonathan P Rourke. A delicate balance of complexation vs. activation of alkanes interacting with [re (cp)(co)(pf3)] studied with nmr and time-resolved ir spectroscopy. *Proceedings of the National Academy of Sciences*, 104(17):6927–6932, 2007.

[20] Wesley H Bernskoetter, Cynthia K Schauer, Karen I Goldberg, and Maurice Brookhart. Characterization of a rhodium (i) σ-methane complex in solution. *Science*, 326(5952):553–556, 2009.

[21] James D Watson, Leslie D Field, and Graham E Ball. Binding methane to a metal centre. *Nature Chemistry*, 14(7):801–804, 2022.

[22] Sebastian D Pike, F Mark Chadwick, Nicholas H Rees, Mark P Scott, Andrew S Weller, Tobias Kraemer, and Stuart A Macgregor. Solid-state synthesis and characterization of σ-alkane complexes,[rh (l2)(η2, η2-c7h12)][barf4](l2= bidentate chelating phosphine). *Journal of the American Chemical Society*, 137(2):820–833, 2015.

[23] F Mark Chadwick, Tobias Kraemer, Torsten Gutmann, Nicholas H Rees, Amber L Thompson, Alison J Edwards, Gerd Buntkowsky, Stuart A Macgregor, and Andrew S Weller. Selective c–h activation at a molecular rhodium sigma-alkane complex by solid/gas single-crystal to single-crystal h/d exchange. *Journal of the American Chemical Society*, 138(40):13369–13378, 2016.

[24] Daniel R Evans, Tatiana Drovetskaya, Robert Bau, Christopher A Reed, and Peter DW Boyd. Heptane coordination to an iron (ii) porphyrin. *Journal of the American Chemical Society*, 119(15):3633–3634, 1997.

[25] Matthew R Gyton, M Arif Sajjad, Daniel J Storm, Kristof M Altus, Joe C Goodall, Chloe L Johnson, Samuel J Page, Alison J Edwards, Ross O Piltz, Simon B Duckett, et al. An operationally unsaturated iridium-pincer complex that c–h activates methane and ethane in the crystalline solid-state. *Journal of the American Chemical Society*, 147(10):8706–8719, 2025.

[26] AA Bengali, Richard H Schultz, C Bradley Moore, and Robert G Bergman. Activation of the ch bonds in neopentane and neopentane-d12 by (. eta. 5-c5 (ch3) 5) rh (co) 2: Spectroscopic and temporal resolution of rhodium-krypton and rhodium-alkane complex intermediates. *Journal of the American Chemical*

Society, 116(21):9585–9589, 1994.

[27] Richard H Schultz, AA Bengali, MJ Tauber, Bruce H Weiller, Eric P Wasserman, KR Kyle, C Bradley Moore, and Robert G Bergman. Ir flash kinetic spectroscopy of ch bond activation of cyclohexane-d0 and-d12 by cp* rh (co) 2 in liquid rare gases: Kinetics, thermodynamics, and unusual isotope effect. *Journal of the American Chemical Society*, 116(16):7369–7377, 1994.

[28] Ian JS Fairlamb and Jason M Lynam. Unveiling mechanistic complexity in manganese-catalyzed c–h bond functionalization using ir spectroscopy over 16 orders of magnitude in time. *Accounts of Chemical Research*, 57(6):919–932, 2024.

[29] Peter W Atkins and Ronald S Friedman. *Molecular quantum mechanics*. Oxford university press, 2011.

[30] Thomas A Albright, Jeremy K Burdett, and Myung-Hwan Whangbo. *Orbital interactions in chemistry*. John Wiley & Sons, 2013.

[31] Jean Yves Saillard and Roald Hoffmann. Carbon-hydrogen and hydrogen-hydrogen activation in transition metal complexes and on surfaces. *Journal of the American Chemical Society*, 106(7):2006–2026, 1984.

[32] Attila Szabo and Neil S Ostlund. *Modern quantum chemistry: introduction to advanced electronic structure theory*. Courier Corporation, 1996.

[33] Frank Jensen. *Introduction to computational chemistry*. John wiley & sons, 2017.

[34] M. Born and R. Oppenheimer. Zur quantentheorie der molekeln. *Annalen der Physik*, 389(20):457–484, 1927.

[35] C. C. J. Roothaan. New developments in molecular orbital theory. *Rev. Mod. Phys.*, 23:69–89, Apr 1951.

[36] Hendrik A Kramers and Werner Heisenberg. Über die streuung von strahlung durch atome. *Zeitschrift für Physik*, 31(1):681–708, 1925.

[37] Joachim Stöhr. *The nature of X-rays and their interactions with matter*. Number PUBDB-2024-05989. Springer, 2023.

[38] Paul Adrien Maurice Dirac. The quantum theory of the emission and absorption of radiation. *Proceedings of the Royal Society of London. Series A, Containing Papers of a Mathematical and Physical Character*, 114(767):243–265, 1927.

[39] Enrico Fermi. Quantum theory of radiation. *Rev. Mod. Phys.*, 4:87–132, Jan 1932.

[40] Burton L Henke, Eric M Gullikson, and John C Davis. X-ray interactions: photoabsorption, scattering, transmission, and reflection at e= 50-30,000 ev, z= 1-92. *Atomic data and nuclear data tables*, 54(2):181–342, 1993.

[41] Akio Kotani and Shik Shin. Resonant inelastic x-ray scattering spectra for electrons in solids. *Reviews of Modern Physics*, 73(1):203, 2001.

[42] Werner Heisenberg. Über den anschaulichen inhalt der quantentheoretischen kinematik und mechanik. *Zeitschrift für Physik*, 43(3):172–198, 1927.